

UNDERSTANDING BLACK HOLE MASS ASSEMBLY VIA ACCRETION AND MERGERS AT LATE TIMES IN COSMOLOGICAL SIMULATIONS

ANDREA KULIER¹, JEREMIAH P. OSTRIKER^{1,2}, PRIYAMVADA NATARAJAN³, CLAIRE N. LACKNER^{1,4}, AND RENYUE CEN¹
Draft version March 5, 2019

ABSTRACT

Accretion and merger triggered accretion episodes are thought to primarily contribute to the mass accumulation history of supermassive black holes throughout cosmic time. While this might be the dominant growth mode at high redshifts, at lower redshifts and for the most massive black holes, mergers themselves might add significantly to the mass budget. In this paper, we explore this in two specific yet disparate environments — black holes harbored in member galaxies in a massive cluster and those in a void region. We use merger trees derived from hydrodynamical cosmological simulations of a cluster and void region to examine the growth of supermassive black holes at late times from $4 > z > 0$. Mass gains from gas accretion and BH-BH mergers are tracked as are black holes that remain unmerged and “orbiting” due to insufficient dynamical friction in a merger remnant, as well as those that are ejected due to gravitational recoil. We find that gas accretion remains the dominant source of mass accumulation in almost all of the SMBHs produced; mergers contribute an average of $3.3 \pm 0.2\%$ for all SMBHs in the cluster, and $1.3 \pm 0.2\%$ in the void from $z = 4$ to 0. However, mergers are significant for massive SMBHs, with the contribution from mergers reaching a maximum of 20% in the cluster for black holes with mass around $10^9 M_\odot$. The fraction of central black hole mass from mergers generally increases for larger values of the host galaxy mass: in the void, the fraction is 2% at $M_* = 10^{10} M_\odot$, 5% at $10^{11} M_\odot$, and 9% at $M_* \approx 10^{12} M_\odot$, and in the cluster it is 4% at $M_* = 10^{10} M_\odot$, 13% at $10^{11} M_\odot$, and 21% at $10^{12} M_\odot$. We also find that the total mass in orbiting SMBHs is negligible in the void except for the few most massive BHs, but significant in the cluster, with a median value of $M_{\text{orbiting}} \gtrsim 10^7 M_\odot$ per galaxy for galaxies with stellar mass $M_* > 10^{11.5} M_\odot$. We find that 40% of SMBHs and $\approx 14\%$ of the total SMBH mass^a is found orbiting in the cluster region at $z = 0$. The existence of such a large unmerged mass fraction requires modification of the Soltan argument where these orbiting BHs are unaccounted for. We estimate the correction to the Soltan argument due to such orbiting SMBHs as well as SMBHs ejected via gravitational slingshot effects to be in the range 1.6 – 15%, with a mean value of $7.4 \pm 3.7\%$ in the estimate of the inventory of the integrated accreted mass density of SMBHs. Quantifying the growth due to mergers at these late times, we calculate the total energy output and strain due to gravitational waves emitted by merging SMBHs.

Subject headings: black hole physics — galaxies: nuclei — quasars: general

1. INTRODUCTION

Observations strongly suggest that supermassive black holes are harbored in the centers of almost all massive galaxies (Kormendy & Richstone 1995). The masses of these central black holes are observed to correlate with multiple properties of their host galaxies. The most well-known and studied of these relations is the $M - \sigma$ relation between the mass of the black hole and the velocity dispersion of its host galaxy spheroid (Gebhardt et al. 2000; Ferrarese & Merritt 2000; Tremaine et al. 2002; Gültekin et al. 2009). Relations between the black hole mass and the stellar mass and luminosity of the bulge have also been derived from observations (Marconi & Hunt 2003; Häring & Rix

2004; Beifiori et al. 2012). It has also been claimed that the mass of the central black hole is correlated with galactic properties on scales larger than the bulge, such as the total stellar mass of the galaxy (Cisternas et al. 2011; Bennert et al. 2011; Beifiori et al. 2012), and the mass of the entire host halo (Ferrarese 2002; Volonteri et al. 2011; see however Kormendy et al. 2011; Kormendy & Bender 2011). There is also evidence of increased scatter in some of these relations for low mass galaxies (Greene et al. 2010b; Volonteri et al. 2011; McConnell & Ma 2012). The existence of these correlations suggests interplay between black hole growth and star formation activity in galactic nuclei.

There appears to be a connection between AGN activity and star formation on galactic scales larger than the nucleus as well. The total AGN activity follows roughly the same trend as a function of cosmic redshift as the global star formation rate (Heckman et al. 2004; Merloni et al. 2004; Brusa et al. 2009; Shankar et al. 2009). A correlation has also been found between the luminosity of individual AGN and the star formation luminosity of their host galaxies (Netzer 2009; Chen et al. 2013). It is becoming clear at high redshifts that the global star formation rate tracking AGN activity does not

akulier@princeton.edu

¹ Department of Astrophysical Sciences, Princeton University, Princeton, NJ 08544, USA

² Department of Astronomy, Columbia University, NYC, NY 10027, USA

³ Department of Astronomy, 260 Whitney Avenue, Yale University, New Haven, CT 06511, USA

⁴ Kavli Institute for the Physics and Mathematics of the Universe (WPI), Todai Institutes for Advanced Study, the University of Tokyo, Kashiwa, Japan

^a where the total includes central, orbiting, and ejected SMBHs

imply that these processes occur in tandem in all individual galaxies (Treister et al. 2013, in preparation). While such relations imply that the evolution of a galaxy and its central black hole are intertwined, their exact origin remains uncertain. Several mechanisms have been proposed. One possibility is that the evolution of a galaxy regulates the growth of its central black hole by determining the amount of gas that finally reaches the black hole (Booth & Schaye 2011). However, a SMBH can also regulate the evolution of its host galaxy through energy input via AGN feedback, which may be able to suppress star formation (Maiolino et al. 2012). Dubois et al. (2012) have run recent cosmological simulations including SMBH growth via accretion and mergers, as well as outflows and heating from AGN feedback, and conclude that AGN feedback is necessary to expel gas and suppress star formation. They also argue that AGN feedback is able to transform late-type galaxies into early-types and explain galaxy scaling relations such as the fundamental plane (Dubois et al. 2013a).

It is not known which of the former two processes is dominant. A third explanation of the scaling relations is that some other factor — for instance, the total gas reservoir — regulates both the growth of the SMBH and the evolution of the galaxy. Bournaud et al. (2012) observed a correlation between giant clumps of gas and stars, which are indicative of violent disk instabilities, and AGN activity at $z \sim 0.7$. They propose that the evolution of disk instabilities, which cause gas inflow to the central bulge and SMBH, could produce the observed correlation between star formation and AGN activity (Bournaud et al. 2011). Finally, a purely statistical explanation has been proposed for the existence of these observed correlations based on the idea that repeated mergers of galaxies, which also lead to the eventual mergers of their central black holes, can cause the SMBHs and their hosts to have correlated masses as a consequence of the central limit theorem (Hirschmann et al. 2010). One or a combination of all these mechanisms could be responsible for the observed scaling relations between SMBHs and their hosts. The argument based on the central limit theorem has recently been gaining strength as the evidence accumulates from both observations (van Dokkum et al. 2008) and theory (Oser et al. 2010) that the most massive galaxies grow their stellar components substantially via minor mergers during recent cosmic epochs. This is especially important for massive BCGs (brightest cluster galaxies) in rich clusters (Hausman & Ostriker 1978; Lin et al. 2013). Evidence that BCGs have grown via mergers has been reinforced by a new statistical test (Lin et al. 2010). The impact of the increased frequency of minor mergers for the assembly of the stellar component suggests that they might play an important role in black hole growth as well at late times.

It is widely believed that black hole growth occurs primarily via accretion or merger triggered accretion episodes over cosmic time, although secular evolution driven by stellar evolutionary processes also appears to be important (Ciotti & Ostriker 1997; Ostriker et al. 2010), especially for $z < 2$. In massive galaxies, which have undergone multiple mergers, it is believed that most of the SMBH growth occurs in short accretion episodes fueled by gas flowing into the central region due to the

merger or galactic cooling flows. SMBHs hosted in small galaxies that have not undergone any major mergers must, however, be supplied with gas through some different mechanism, such as dynamical relaxation and perhaps secular evolution processes (Sesana 2012a). While these may indeed be the primary channel of growth during early times, it is becoming evident that the actual merger of black holes might contribute appreciably to the final mass inventory of the most massive black holes at low redshifts. This is suggested by the current evidence that minor mergers are a significant component of the late-time stellar mass growth of the most massive galaxies.

In this paper, we examine how gas inflows, mergers, and the large-scale environment determine black hole growth. To this end we track the growth histories of black holes in a typical over-dense cluster environment and an under-dense void environment. In particular, we know that the merger history in these environments at late times is divergent. Therefore, in this work we focus on quantifying the role that mergers play in the mass assembly history at late times. This has important consequences for the expected gravitational radiation from such events at low redshifts as well the observational implications for the number of wandering black holes. Since BH-BH mergers will be accompanied by the gravitational slingshot effect (Peres 1962; Bekenstein 1973; Fitchett & Detweiler 1984), late time mergers may eject a significant amount of mass in BHs from merged galaxies. An inventory of BHs at the present epoch will, of course, not count this mass and thus will underestimate the $z = 0$ cosmic mass density locked up in SMBHs. Furthermore, we expect that some SMBHs at any given time will be orbiting in the outskirts of the galactic potential — as the result of a lower velocity gravitational wave recoil or a recent merger of its host with a more massive galaxy. These orbiting BHs will also not be found in observations of galactic centers. The correction to the SMBH mass density from these two populations, which we estimate here, implies that the Soltan argument (Soltan 1982) will necessarily overestimate the efficiency of energy output from accreting BHs. This is due to the fact that the energy output from accretion that is directly observed is incommensurate with the SMBH cosmic mass density estimated only from the census of BHs in galactic centers. Neglecting the “unmerged” SMBH population introduces errors in estimates of the inferred accretion efficiency for the population of BHs.

The outline of the paper is as follows: we first briefly summarize relevant previous work on the evolution of supermassive black holes in §2. We then describe the key aspects of the problem that are tackled here — the role of late time mergers — in §3. In §4, the methodology and cosmological simulations used are detailed, followed by the analysis and results in §5. We conclude with a discussion of the implications and observational consequences of accounting for the role of minor mergers at late times on our current understanding of black hole growth.

2. PREVIOUS WORK

The evolution of supermassive black holes through cosmic time has been modeled using different approaches by tracking the dark matter halos they reside in, including

Monte Carlo merger trees (e.g., Haehnelt & Kauffmann 2000; Lippai et al. 2009; Natarajan 2011), Press-Schechter theory (e.g., Yoo et al. 2007), and cosmological simulations (e.g., Di Matteo et al. 2003; Sijacki et al. 2009). A more complete review of the early models of the growth of SMBHs is given in Natarajan (2004).

Simulations of the evolution of black hole scaling relations have been done both semi-analytically (e.g., Kisaka & Kojima 2010) and numerically (e.g., Johansson et al. 2009). Most studies have focused on understanding black hole growth in individual galaxies residing in average over-density environments, typically the field. There have been few studies of black hole mass assembly in extremely over-dense cluster and under-dense void environments. Using dark matter merger trees derived from Press-Schechter theory, Yoo et al. (2007) examined the expected growth of black holes due to mergers in a large cluster with halo mass $M_h = 10^{15} h^{-1} M_\odot$ at late times. They found that most SMBHs in the cluster with masses $\gtrsim 10^{7.5} M_\odot$ underwent mergers, with the most massive SMBHs increasing their mass by a factor of ~ 2 since $z = 2$. Although the central galaxy generally contained the most massive SMBH at $z = 0$, Yoo et al. (2007) found that for some cluster assembly histories, the most massive SMBH may be hosted by a satellite galaxy.

Current simulations do not agree on the evolution of BH-galaxy scaling relations with redshift. Some find that SMBHs at higher z should be more massive than they would be if they followed the current $M - \sigma$ relation (Hopkins et al. 2009; Dubois et al. 2012), while others find that they should be less massive (Malbon et al. 2007; Di Matteo et al. 2008). Observations at redshifts up to $z \sim 4$ seem to indicate that the $M - \sigma$ relation changes such that SMBHs are more massive at fixed velocity dispersion than those in the present day (McLeod & Bechtold 2009; Woo et al. 2008; Greene et al. 2010a; see however Shields et al. 2003; Zhang et al. 2012). Others observations have looked at the $M - M_{*,\text{spheroid}}$ and $M - M_{*,\text{host}}$ relationships, and similarly have argued for evidence supporting an increase in black hole mass at fixed host mass with increasing redshift (Bennert et al. 2011; Merloni et al. 2010; Zhang et al. 2012).

Complementary constraints on BH growth models can be derived from X-ray luminosity functions of AGN. Since X-rays can escape even the most obscured Compton-thick galactic nuclear sources, they offer a unique probe of actively growing BHs (Salvaterra et al. 2007). Several studies that have attempted to explain the origin of the cosmic X-ray background have also provided insights into both the obscured and unobscured accreting populations of BHs over cosmic time (c.f. models by Gilli et al. 2007; Treister et al. 2009). Relevant to our study are the constraints obtained by Volonteri et al. (2006) on the accretion history of SMBHs at $z < 3$ using observations of the faint X-ray background combined with optical and hard X-ray luminosity functions. They found that a model in which the Eddington ratio is a function of the AGN luminosity — as suggested by previous simulations — fits the observational constraints somewhat better than models with a constant Eddington ratio or an Eddington ratio decreasing with redshift.

As for the population of “wandering” black holes, the buildup of populations of orbiting and ejected

black holes as a result of galaxy mergers and gravitational wave recoils has been examined most recently by Rashkov & Madau (2013). Although their approach bears similarities to ours, they studied the evolution of intermediate-mass black holes (IMBHs), which are thought to be the ancestral seeds of the supermassive black holes currently found in the centers of galaxies. They populated the N-body *Via Lactea II* cosmological simulation of a Milky Way-size halo (Diemand et al. 2008) with seed IMBHs, which they then allowed to evolve via mergers and gravitational wave recoils. They found that even when assuming “maximal” numbers of BHs would escape the galaxy due to gravitational wave kicks, a sizable population of leftover IMBHs should be orbiting in the halo of a galaxy with the mass of the Milky Way. We focus on slightly different mass scales in this work and examine the status of the growth of the central SMBH and the SMBH wanderers in a typical cluster rather than a galaxy scale halo.

3. EXPLORING THE ROLE OF LOW-REDSHIFT MERGERS

In this paper, we examine the consequences of mergers for the mass assembly history of SMBHs at late times and the observational consequences thereof. The energy released during black hole assembly over cosmic time has been estimated by integrating the energy output of observed AGN (Soltan 1982). This argument made by Soltan employs the observed luminosity function of quasars and requires an estimate of the total mass in black holes per unit cosmic volume, which was assumed thus far to not be significantly altered by mergers among black holes (Menou & Haiman 2004). However, mergers in cluster environments at late times are ubiquitous and these events will produce gravitational waves, and the amount of energy released in them is important to know accurately for detection experiments (McWilliams et al. 2012). Using the Soltan argument, the SMBH mass density has been found to be consistent with the luminosity density of QSOs if these QSOs have a mass-to-energy conversion efficiency of $\epsilon \simeq 0.1$ (Yu & Tremaine 2002). Taking mergers explicitly into account, including ejections will alter the observational consequences at low redshifts and that is precisely what we explore in detail in this paper. Thus far the total energy that is emitted in gravitational waves has been estimated using primarily Monte-Carlo dark matter merger trees; however, these approaches do not take into careful account the enhanced merger rates in cluster environments where the most massive galaxies live (Sesana 2012b).

We note that not all galactic mergers will result in black hole mergers, due to a finite dynamical friction time for the black hole to sink to the center of the galactic potential. Also, there exists the “final parsec problem” (see e.g., Milosavljević & Merritt 2003), which is shorthand for the physical difficulties in bridging the gap between the binary separation reached by dynamical friction between the SMBH and the ambient stellar population and the much smaller separation at which gravitational radiation takes over as the primary angular momentum loss mechanism for the BH binary. We will not address this problem in this paper, but will assume that black holes effectively merge at galactic centers on the dynamical friction timescale.

In this work, we use recent cosmological simulations

(Cen 2011a,b, 2012a,b, 2013) to explore the relevance of different processes on the growth of SMBHs and their implications for the setting up of the various observed scaling relations in two significantly different environments. In our book-keeping we keep track of the total mass in black holes in the following four categories at redshifts between $z = 4$ and 0:

- The mass in central black holes acquired from accretion of gaseous matter.
- The mass in central black holes acquired from mergers with smaller black holes.
- The mass in orbiting black holes that have not yet fallen to the center of the galactic potential.
- The mass in ejected black holes that have been kicked out due to gravitational radiation recoil.

The final two categories will be assessed as corrections to the normal Soltan-type arguments for estimating the revised efficiency of BH-associated energy generation.

4. METHODOLOGY AND DESCRIPTION OF COSMOLOGICAL SIMULATIONS

As the basis for our analysis of SMBH evolution, we use the large-scale hydrodynamical galaxy simulations of Cen (2011a,b, 2012a,b, 2013). Detailed descriptions of the simulations can be found in the papers referenced above; we provide a brief overview in this section. We use galactic (not dark matter based) merger trees derived from these simulations as described in Lackner et al. (2012). The simulations are performed with the AMR (Adaptive Mesh Refinement) Eulerian hydrodynamics code, Enzo (Bryan 1999; O’Shea et al. 2004; Joung et al. 2009). They consist of a low-resolution box of $120 h^{-1}$ Mpc on a side, and two high-resolution regions within this box, one containing a cluster with mass $\sim 3 \times 10^{14} M_{\odot}$, and the other a void. These represent $+1.8\sigma$ and -1.0σ fluctuations in the cosmic density field, respectively. These two extreme regions bracket the cosmic average environment. The cluster region box has dimensions $21 \times 24 \times 20 h^{-3} \text{ Mpc}^3$, and the void box has dimensions $31 \times 31 \times 35 h^{-3} \text{ Mpc}^3$. The dark matter particle mass is $1.07 \times 10^8 h^{-1} M_{\odot}$, while the stellar particle mass is generally around $10^6 M_{\odot}$. The resolution in the cluster and void regions is always better than $460 h^{-1} \text{ pc}$ physical.

The simulation includes prescriptions for UV background (Haardt & Madau 1996), shielding from UV radiation by neutral hydrogen (Cen et al. 2005), metallicity-dependent radiative cooling (Cen et al. 1995), formation of star particles from gas (Cen & Ostriker 1992), and supernovae feedback (Cen et al. 2005). It does not include feedback from AGN, which may be partly the reason that the largest galaxies in the simulation box have too many stars in comparison with observed relations. This is a well known problem in hydrodynamical simulations (Oser et al. 2010; Guo et al. 2010) and one that does exist in our version.

The simulations use the following cosmological parameters, consistent with Komatsu et al. (2009): $\Omega_M = 0.28$, $\Omega_b = 0.046$, $\Omega_{\Lambda} = 0.72$, $\sigma_8 = 0.82$, $H_0 = 100h^{-1} \text{ Mpc}^{-1} = 70 \text{ km s}^{-1} \text{ Mpc}^{-1}$, and $n = 0.96$. These are also the values we adopt throughout this paper in our calculations.

Galaxies in the simulation box are identified by using the HOP algorithm on stellar particles (Eisenstein & Hu 1999). The following are some of the physical parameters calculated and tracked for each galaxy: position, velocity, total mass, stellar mass, gas mass, mean formation time, mean stellar metallicity, mean gas metallicity, star formation rate, and luminosities and colors for five SDSS bands, among others. In general, broad agreement is found between the simulation results and observations (Cen 2011a).

A merger tree is created from this simulation. In the cluster box, there are 38 redshift slices from $z = 4$ to $z = 0$ with $\Delta z = 0.05$ for $z < 1.35$, and slices at $z = 1.5, 1.6, 1.75, 1.9, 2.0, 2.2, 2.5, 2.8, 3.1$, and 4. In the void box, there are 14 redshift slices between $z = 0$ and $z = 4$, at $z = 0, 0.05, 0.15, 0.2, 0.4, 0.5, 0.6, 0.8, 1.0, 1.6, 1.9, 2.5, 3.1$ and 4 (Lackner et al. 2012). We seed the galaxies in this merger tree with central black holes and trace their evolution based on the evolution of their host galaxies. Further details are provided below.

4.1. Black Hole Evolution Prescriptions

Since our focus is on massive galaxies, we use galaxies from the simulation only if they have stellar masses $M_* > 10^9 M_{\odot}$, due to the resolution limit of the simulation. In the cluster box, all galaxies above this mass limit have descendants at $z = 0$. In the void box, the grouping algorithm identifies some groupings of particles above this mass limit as galaxies that do not exist in the next redshift slice. For our purposes, we ignore any groupings of particles that do not have a descendant at $z = 0$.

We place a seed black hole in any galaxy that reaches the lower mass limit of $10^9 M_{\odot}$ at any redshift. The seed black hole is taken to have mass nM_* , where n is selected from a log-normal distribution with median value 10^{-3} . This matches the approximate observed mass ratio of the SMBH to its host galaxy bulge (Volonteri 2012), and is based on the assumption that of the gas added to (and retained by) galaxies, approximately one part in a thousand is accreted onto the central black hole, with most of the remainder transformed into stars (Li et al. 2007). It is widely believed that AGN feedback helps to limit the growth of the central black hole, and some simulations (Hopkins & Hernquist 2009; Ostriker et al. 2010; Park & Ricotti 2012) indicate that this is likely. We note that this assignment of BH seed masses as early as $z = 4$ pre-supposes the existence of a scaling relation at this epoch akin to what is empirically measured at $z = 0$.

SMBHs are then allowed to grow through BH-BH mergers and accretion of gaseous material from the galaxy. We calculate the accreted and merged mass by considering all parent black holes of a single black hole to be “merged mass” except for the most massive one. We adopt a simple prescription for accretion in which the mass accreted by the central black hole in each redshift slice is proportional to the amount of stars

formed in the galaxy in that redshift slice, with some scatter in the assumed proportionality factor. Because stars are sometimes ejected from galaxies in the simulation, it is possible for the total stellar mass of a galaxy to occasionally decrease. If this is the case, we assume zero accretion onto the black hole in that redshift slice. Otherwise, the mass accreted by the black hole is taken to be $n'\Delta M_{\text{insitu}}$, where ΔM_{insitu} is the change in galaxy stellar mass due to star formation in that redshift slice, and n' is a proportionality factor chosen from the same log-normal distribution as the proportionality factor for the seeding prescription. We choose this accretion rate in order to match the observed correlation between AGN activity and galactic star formation rate (Heckman et al. 2004; Merloni et al. 2004; Brusa et al. 2009; Shankar et al. 2009). Because the luminosity of an AGN is determined by its growth rate due to accretion, these data imply that AGN grow at a rate roughly proportional to the rate of star formation in their host galaxy, with a proportionality factor of about 10^{-3} . We adjust the scatter of the log-normal distribution from which the proportionality factor for the seed masses and BH accretion rate is chosen so as to produce a scatter of ~ 0.4 in the cluster $M_{\bullet} - M_*$ relation at $z = 0$, similar to observed values reported in the literature (Bennert et al. 2011; Hu 2009; McConnell & Ma 2012).

Because we fix the relations of seed mass to host galaxy mass and accreted mass to star formation to be the same at all redshifts, we essentially force the $M_{\bullet} - M_*$ to be constant with redshift. Accounting for ejected and orbiting BHs can cause some evolution in the relation by lowering the central BH mass compared to the $M_{\bullet} - M_*$ relation, but, as will be described in the results (§5), the change in mass from these effects is on average rather small. Thus our model does not account for the evolution in the BH-galaxy scaling relations seen in some previous work (e.g., Merloni et al. 2010; Zhang et al. 2012).

When a smaller galaxy merges into a larger one, we calculate the dynamical time for the black hole from the smaller galaxy to move to the center of the newly formed merged galaxy. We use the dynamical friction formula of Binney & Tremaine (1987):

$$t_{\text{DF}} = \frac{19 \text{ Gyr}}{\ln(1 + M_*/M_{\bullet})} \left(\frac{R_e}{5 \text{ kpc}} \right)^2 \frac{\sigma}{200 \text{ km/s}} \frac{10^8 M_{\odot}}{M_{\bullet}}. \quad (1)$$

We obtain values for the velocity dispersion σ and effective radius R_e of our simulated galaxies by using observed fits to the mass from SDSS data (Nipoti et al. 2009), and redshift dependences from Oser et al. (2010):

$$R_e = 2.5 \text{ kpc} \left(\frac{M_*}{10^{11} M_{\odot}} \right)^{0.73} (1+z)^{-1.44}, \quad (2)$$

$$\sigma(R_e) = 190 \text{ km/s} \left(\frac{M_*}{10^{11} M_{\odot}} \right)^{0.2} (1+z)^{0.44}. \quad (3)$$

If a galaxy is involved in another merger before a satellite black hole has merged with the central one, we recalculate the dynamical friction time. If the satellite black hole is in the more massive galaxy, we take the new dynamical friction time to be the smaller of the remaining time to black hole merger and the dynamical friction time that would be calculated for the post-merger galaxy. For

a less massive galaxy merging into a more massive one, its satellite and central black holes are taken to have a dynamical friction time calculated for the new post-merger galaxy. In this way, we keep track of both central and satellite SMBHs in galaxies.

If a black hole is ejected or displaced from the center of a galaxy due to a gravitational wave recoil (see §4.2.1 below), the galaxy may have no central SMBH. If a galaxy lacking a central BH produces and additional $10^9 M_{\odot}$ in star formation, we seed it again with a black hole with mass proportional to the mass in stars formed, where the proportionality constant is chosen from the same log-normal distribution as for the seeds and accreted mass described earlier.

4.2. Low redshift merging and gravitational radiation

We calculate the gravitational radiation luminosity expected based on the BH-BH mergers that occur in our simulation. This energy is equivalent to the mass lost from the black hole pair as they are merging. For each BH-BH merger, we apply an approximation for the energy emitted in gravitational waves taken from Barausse et al. (2012):

$$\frac{E_{\text{rad}}}{M} = [1 - \tilde{E}_{\text{ISCO}}(\tilde{a})]\nu + 4\nu^2[4p_0 + 16p_1\tilde{a}(\tilde{a} + 1) + \tilde{E}_{\text{ISCO}}(\tilde{a} - 1)]. \quad (4)$$

Here $M \equiv m_1 + m_2$ is the total mass of the two black holes and $\nu \equiv m_1 m_2 / M^2$ is the symmetric mass ratio. The constants p_0 and p_1 come from a polynomial fit to the energy emitted by inspiraling binary black holes, and have the values:

$$p_0 = 0.04827 \pm 0.00039, \quad p_1 = 0.01707 \pm 0.00032. \quad (5)$$

Here \tilde{E}_{ISCO} is the energy per unit mass at the innermost stable circular orbit and is given by:

$$\tilde{E}_{\text{ISCO}}(\tilde{a}) = \sqrt{1 - \frac{2}{3\tilde{r}_{\text{ISCO}}^{\text{eq}}}(\tilde{a})}, \quad (6)$$

where

$$\begin{aligned} \tilde{r}_{\text{ISCO}}^{\text{eq}}(\tilde{a}) &= 3 + Z_2 \\ &\quad - \text{sign}(\tilde{a})\sqrt{(3 - Z_1)(3 + Z_1 + 2Z_2)}, \\ Z_1 &= 1 + (1 - \tilde{a}^2)^{1/3} \left[(1 + \tilde{a})^{1/3} + (1 - \tilde{a})^{1/3} \right], \\ Z_2 &= \sqrt{3\tilde{a}^2 + Z_1^2}. \end{aligned} \quad (7)$$

In all the above equations, \tilde{a} is defined as

$$\tilde{a} \equiv \frac{\hat{\mathbf{L}} \cdot (\mathbf{S}_1 + \mathbf{S}_2)}{M^2} = \frac{|\mathbf{a}_1| \cos \beta + q^2 |\mathbf{a}_2| \cos \gamma}{(1 + q)^2}, \quad (8)$$

where $q \equiv m_2/m_1 < 1$ is the mass ratio of the two black holes, $|\mathbf{a}_1|$ and $|\mathbf{a}_2|$ are the spin magnitudes, and β and γ are the angles between the orbital angular momentum unit vector $\hat{\mathbf{L}}$ and the spins of the first and second black hole, respectively.

By construction, this formula is accurate in both the test-particle limit and for equal-mass binaries. The expected spin vector distribution of SMBHs and its evolution are not well agreed upon in the literature (see

e.g., Volonteri et al. 2005; Barausse 2012; Dubois et al. 2013b). Thus, we make the most “simple” possible assumption by selecting spin parameter values from a random uniform distribution between 0 and 1, and the cosine of the angles between the spins and the orbital angular momentum from a uniform random distribution between -1 and 1. This is similar to the assumptions made by Schnittman & Buonanno (2007) when calculating the expected recoil velocity distribution of SMBHs.

4.2.1. Gravitational Wave Recoils

When two orbiting supermassive black holes merge, the gravitational radiation produced can impart a linear (“slingshot”) momentum to the SMBH resulting from the merger (Peres 1962; Bekenstein 1973; Fitchett & Detweiler 1984). Recent numerical simulations of general relativity show that such “kicks” can in some cases be large enough to exceed the escape velocity of the host galaxy and eject the resulting SMBH (Herrmann et al. 2007; Koppitz et al. 2007; Campanelli et al. 2007a,b; Lousto & Zlochower 2011). Gravitational wave recoils with velocities insufficient to eject the SMBH can still displace it from the center of the galaxy, to which it may return via dynamical friction.

As we noted earlier, ejections of SMBHs are particularly important as they could alter the quasar efficiency determined from the classic “Soltan argument” (Soltan 1982). This argument assumes that the infall of mass onto quasars over the history of the universe can be integrated over the local galaxy population to give the observed mass density of SMBHs in the local universe. Since quasar luminosities are proportional to their mass growth rates — $L = \epsilon \dot{M} c^2$, where ϵ is the efficiency factor — observations of the total luminosity from quasars can be used to find the efficiency factor ϵ (Yu & Tremaine 2002; Marconi et al. 2004). However, if a significant fraction of SMBHs are ejected from their hosts, then there is less mass in galactic center SMBHs today than was produced in quasars in the past, and the efficiency obtained from the Soltan argument is an overestimate.

We account for the effects of gravitational wave “kicks” on our population of SMBHs, including both ejections and displacements from the center of the galaxy. We use the fitting formula based on numerical simulations from Lousto et al. (2012) for the velocity imparted to an SMBH resulting from a merger:

$$\begin{aligned} \mathbf{V}_{\text{recoil}}(q, \boldsymbol{\alpha}) &= v_m \hat{\mathbf{e}}_1 + v_{\perp} (\cos \xi \hat{\mathbf{e}}_1 + \sin \xi \hat{\mathbf{e}}_2) + v_{\parallel} \hat{\mathbf{n}}_{\parallel}, \\ v_m &= A_m \frac{\eta^2 (1 - q)}{(1 + q)} [1 + B_m \eta], \\ v_{\perp} &= H \frac{\eta^2}{(1 + q)} [(\alpha_2^{\parallel} - q \alpha_1^{\parallel})], \\ v_{\parallel} &= 16 \eta^2 / (1 + q) [V_{1,1} + V_A \tilde{S}_z + V_B \tilde{S}_z^2 + V_C \tilde{S}_z^3] \\ &\times |\boldsymbol{\alpha}_2^{\perp} - q \boldsymbol{\alpha}_1^{\perp}| \cos(\phi_{\Delta} - \phi_1). \end{aligned} \quad (9)$$

Here $\eta = q/(1 + q)^2$, where $q = m_1/m_2$ is the mass ratio of the smaller to larger black hole, $\boldsymbol{\alpha}_i = \mathbf{S}_i/m_i^2$ is the dimensionless spin of black hole i , \parallel and \perp refer to components parallel and perpendicular to the orbital angular momentum, respectively, $\hat{\mathbf{e}}_1$ and $\hat{\mathbf{e}}_2$ are orthogonal unit vectors in the orbital plane, ξ is the angle between the un-

equal mass and spin contribution to the recoil velocity in the orbital plane and $\tilde{\mathbf{S}} = 2(\boldsymbol{\alpha}_2 + q^2 \boldsymbol{\alpha}_1)/(1 + q)^2$. $\phi_{\Delta} - \phi_1$ is the angle between $\boldsymbol{\Delta}^{\perp} = M(\mathbf{S}_2^{\perp}/m_2 - \mathbf{S}_1^{\perp}/m_1)$ and some fiducial direction at merger. The coefficients are obtained numerically and are $H = 6.9 \times 10^3$, $A_m = 1.2 \times 10^4$, $B_m = -0.93$, $V_{1,1} = 3677.76$ km/s, $V_A = 2481.21$ km/s, $V_B = 1792.45$ km/s, and $V_C = 1506.52$ km/s (Lousto et al. 2012). This formula is similar to those obtained by previous authors, e.g. Campanelli et al. (2007a); Baker et al. (2008); van Meter et al. (2010). We assume randomly distributed spin magnitudes and spin directions with respect to the orbital angular momentum as described in §4.2.

To calculate the trajectory of the kicked SMBH, we follow a similar prescription as Madau & Quataert (2004): we assume the density profile of the galaxy is a truncated isothermal sphere, with a core radius equal to the radius of gravitational influence of the post-merger SMBH, $R_{\text{BH}} \approx GM_{\text{BH}}/\sigma^2$, so that $\rho(r) = \sigma^2/[2\pi G(r^2 + R_{\text{BH}}^2)]$. The velocity dispersion σ is obtained from Equation 3. If the $|\mathbf{V}_{\text{recoil}}|$ from gravitational wave radiation is found to be larger than the isothermal sphere escape speed $2\sigma(\ln(R_e/R_{\text{BH}}))^{1/2}$, where the effective radius R_e is obtained from Equation 2, we assume the black hole is ejected from the galaxy. If the kick is insufficient to eject the black hole, we calculate the time for the displaced SMBH to return to the center of the galaxy via dynamical friction. We approximate the orbits of the kicked BHs as purely radial, and calculate their radii as a function of time numerically. This generally results in a dynamical friction timescale that is significantly shorter than that for circular orbits, which is the assumption we use when calculating the dynamical friction timescale of a SMBH after the merger of its host galaxy with a more massive galaxy.

We solve numerically for the radial position of the SMBH as a function of time on a radial orbit using the equation of dynamical friction

$$\begin{aligned} \frac{d^2 \mathbf{r}}{dt^2} &= -\frac{GM(r)}{r^2} \hat{\mathbf{r}} \\ &- \frac{4\pi G^2 \rho M_{\text{BH}} \ln \Lambda}{v^2} \left(\text{erf}(x) - \frac{2x}{\sqrt{\pi}} e^{-x^2} \right) \hat{\mathbf{v}}, \end{aligned} \quad (10)$$

where $M(r)$ is the mass within radius r , $x = v/\sqrt{2}\sigma$, and the Coulomb logarithm $\ln \Lambda$ is taken to be equal to 1, for reasons described in Madau & Quataert (2004) and Maoz (1993). It should be noted that the dynamical friction times for radial orbits are highly dependent on the assumed central density (or equivalently, core radius), and so are only a rough approximation.

4.3. Scaling of Cluster and Void Boxes

Our simulation considerably overproduces stellar mass compared to the amount of dark matter present. This is a common problem in cosmological simulations (Oser et al. 2010; Guo et al. 2010). As described above, our prescriptions for the growth of the central BH are such that the mass of the BH must be nearly proportional to the stellar mass of its host. Thus the excess stellar mass per unit cosmic volume in our simulations also implies an excess of BH mass. We attempt to allow for this in a simple way by scaling down our results for the cluster and void boxes

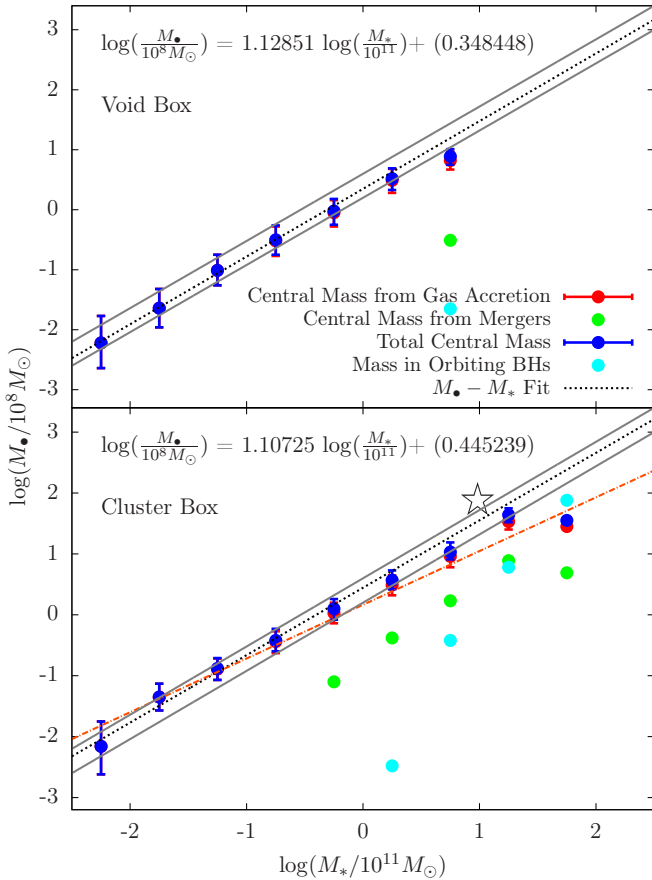


FIG. 1.— $M_{\bullet} - M_{\star}$ relation at $z = 0$. The points are median masses and the error bars represent one quartile. We plot the median BH mass per galaxy in four categories: the total mass of the central SMBH (M_{\bullet}), the amount of mass in the central SMBH that was accreted from galactic gas, the amount of central SMBH mass from mergers with less massive SMBHs, and the total amount of mass found in SMBHs that are orbiting in the galaxy. The black dashed line is a fit to $M_{\bullet} - M_{\star}$ for *all* the galaxies in each simulation box (not only the displayed median points), and the resulting relation is displayed on the plot. Gray solid lines are two different $M_{\bullet} - M_{\star}$ relations from observational data; the upper one is from Bennert et al. (2011), the lower one from Cisternas et al. (2011). The orange dot-dashed line is a fit to $M_{\bullet} - \sigma$ data from the Virgo cluster from Ferrarese et al. (2006), converted to $M_{\bullet} - M_{\star}$ using Equation 3. The star symbol represents the position of M87 and its SMBH (Gebhardt & Thomas 2009; Forte et al. 2012) marked as a reference.

in proportion to the excess of star formation efficiency.

In the cluster, the stellar mass is $3 \times 10^{13} M_{\odot}$ within r_{200} , the radius within which the mean density is equal to 200 times the critical density. The dark matter mass within this same radius is $3 \times 10^{14} M_{\odot}$ (Lackner et al. 2012). This implies a stellar to dark matter ratio of 0.1 within the virial radius. Comparing this to the stellar-halo mass relation found by Leauthaud et al. (2012) using weak lensing and halo occupation distribution methods, combined with the fraction of halo mass that is in gas given by Pratt et al. (2009), one finds that our simulation overproduces stars for a cluster of this mass by a factor of roughly 4 to 6. Determinations of the stellar-halo mass relation found by matching simulated dark matter halos to observed galaxy mass functions (Guo et al. 2010; Behroozi et al. 2010; Moster et al. 2013) find somewhat lower values than

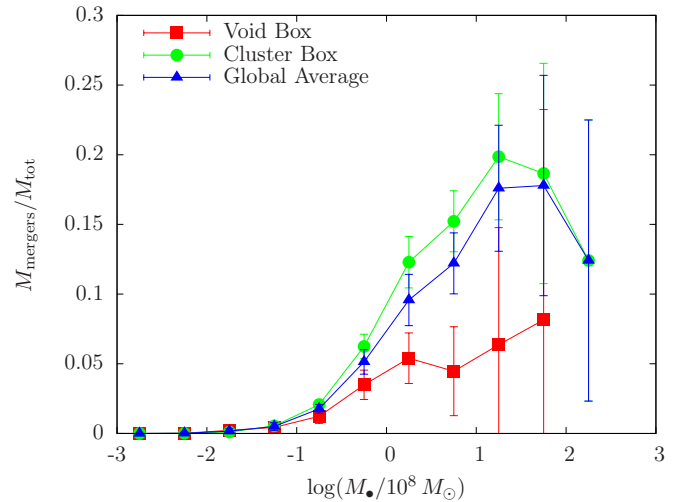


FIG. 2.— The number-weighted mean fraction of total central SMBH mass gained via BH mergers as a function of SMBH mass at $z = 0$. Error bars are 1σ . Values are shown for BHs in the void and cluster boxes as well as for an approximate “global average” combination of the two (see §4.3).

Leauthaud et al. (2012), implying an even larger excess for our simulation. Recent observational determinations of low redshift cluster stellar masses using WISE and 2MASS and halo masses using *Chandra* find values of the stellar to dark matter ratio in the range $\approx 0.01 - 0.03$ (Lin et al. 2012). This corresponds to an overproduction of stellar mass by a factor of 3 to 10. Given these results, we choose a scaling factor for the cluster of 1/5. This factor is applied to both galaxy and black hole masses. Further, all predicted observables are scaled down in the way in which they are proportional to the BH or galaxy mass; e.g. the luminosity due to accretion of gas by the BH, which is directly proportional to the growth of the BH mass, is scaled by 1/5, whereas the square of the gravitational wave strain h_c^2 , which is proportional to $M_{\bullet}^{5/3}$ (see Equations 11 and 12), is scaled by $(1/5)^{5/3}$.

Given the lack of observational data for the star formation efficiency specifically in the void, we assume arbitrarily that the stellar to dark matter mass ratio in the void is half of the mean ratio of the universe. We calculate the mean universal value using the $z = 0$ stellar mass density from Muzzin et al. (2013), who combined the Kroupa IMF with measurements from Cole et al. (2001), Bell et al. (2003), and Baldry et al. (2012) to obtain $\rho_{\star} = 3.07 \times 10^8 M_{\odot} \text{ Mpc}^{-3}$. This results in a mean stellar to dark matter mass ratio of 0.00967, and thus a ratio of 0.00484 for the void. The stellar to dark matter ratio for the entire void box in our simulation is 0.012 (Lackner et al. 2012), so we scale the results we obtain for the void by a factor of 2/5 in the same manner that we do for the cluster.

It should be noted that these scalings for the void and cluster box are simple and do not reflect the more complex trends in stellar mass production in our simulation. In particular, our simulation does not overproduce stellar mass equally for all galaxies, but instead produces a galaxy stellar mass function whose shape does not match observations. The simulation overproduces very massive galaxies and underproduces low-mass galaxies, especially in the cluster box. Also, the most massive galax-

ies are over-merged. Detailed comparison of our galaxy stellar mass function with observations can be found in Lackner et al. (2012).

The cluster and void boxes in the cosmological simulation we use are $+1.8\sigma$ and -1σ fluctuations in the cosmic density field, respectively, and were chosen so as to bracket the “global average” of various physical quantities (Cen 2011a). To approximate this global average, we combine the rescaled quantities from the void and cluster boxes in a weighted average. We choose weights such that the average stellar mass density at $z = 0$ is equal to $3.07 \times 10^8 M_\odot \text{Mpc}^{-3}$, the observed local stellar mass density. Although we only count galaxies with stellar masses greater than $10^9 M_\odot$, galaxies with masses below this mass limit should contribute negligibly to the total stellar mass density (Brinchmann et al. 2004). This results in a weight of 19% (per unit volume) for the cluster box and 81% for the void box. We apply these weights at all redshifts.

All the results given in this paper for the void and cluster boxes are scaled by the aforementioned factors of $2/5$ and $1/5$, respectively, unless explicitly stated otherwise. The global average is the weighted average of the scaled void and cluster values. Because the scaling factors are constant for all masses and redshifts, it is simple to reobtain the original results from our model, or to calculate results for a different preferred normalization.

We also run multiple realizations of our randomized model and use them to compute one-sigma errors on the results we obtain. However, it should be noted that although our black hole growth is modeled with random scatter, we are always using the same galaxy merger trees obtained from the simulations of Cen (2011a).

5. RESULTS

In this section, we present the results of following the SMBH evolution in both the cluster and void environments. Figure 1 shows the black hole mass in different categories versus the galaxy stellar mass in the void and cluster boxes. Our simulations reproduce the empirically observed trend of central black hole mass with stellar mass. Shown for comparison are $M_\bullet - M_*$ relations from Ferrarese et al. (2006), Cisternas et al. (2011), and Bennert et al. (2011). We find that in the cluster environment for the most massive black holes a larger fraction of their mass growth occurs due to direct black hole mergers compared to lower mass black holes. In the void box, where there are on average fewer mergers, the median contribution of direct mergers to the mass inventory of BHs is zero except for the most massive bin, in which it is still lower than for BHs of the same mass in the cluster box.

For the same reason, the amount of mass in BHs orbiting in galaxies in the void box is negligible with the exception of the largest mass bin, as opposed to in the cluster box, where the orbiting mass is substantial for galaxies with $M_* \gtrsim 10^{11} M_\odot$. It should be noted that due to the way we scale down our galaxy and BH masses (§4.3), the number of orbiting black holes will be overestimated for the scaled-down mass range, since the dynamical friction time (Equation 1) for the BHs to spiral in is calculated based on the unscaled mass of galaxies in our model. However, even for the original masses a substantial number of orbiting BHs are predicted for galaxies

of reasonable masses; in the cluster box, ~ 3 orbiting SMBHs are expected for each galaxy with (unscaled) mass $10^{12} M_\odot$, with the number increasing for larger masses. For the void box, the number for a $10^{12} M_\odot$ galaxy is ~ 0.6 orbiting BHs per galaxy; galaxies with this original mass are among the most massive in the void.

The difference between the fraction of BH mass contributed by mergers in the void and cluster boxes is shown more clearly in Figure 2. The number-weighted mean mass fraction from mergers is essentially zero for SMBHs with mass less than $10^7 M_\odot$ in both boxes and increases for larger masses. For the cluster, the fraction reaches a maximum of 20% for BHs with masses around $10^9 M_\odot$. For BHs with larger masses, the fraction decreases to about 12%, although the values have high scatter. In the void, the fraction reaches about 8% for the most massive BHs ($M_\bullet \gtrsim 10^{9.5} M_\odot$). The fraction of central black hole mass from mergers can also be examined as a function of the host galaxy mass. The contribution from mergers is negligible for host masses $M_* \lesssim 10^{9.5} M_\odot$ in both the void and cluster boxes. It increases with host mass such that in the void the fraction of BH mass from mergers is 2% at $M_* = 10^{10} M_\odot$, 5% at $10^{11} M_\odot$, and 9% for the most massive galaxies in the void, which have masses $10^{11.5} M_\odot \lesssim M_* \lesssim 10^{12} M_\odot$. In the cluster box, the fraction from mergers is 4% at $M_* = 10^{10} M_\odot$, 13% at $10^{11} M_\odot$, and 21% at $10^{12} M_\odot$. The fraction drops slightly in the cluster for $M_* > 10^{12.5} M_\odot$, likely due to the long dynamical friction time in such massive galaxies that causes orbiting BHs to accumulate instead of merging with the central BH. The number-weighted mean mass contribution from mergers for all SMBHs is $1.3 \pm 0.2\%$ in the void box and $3.3 \pm 0.2\%$ in the cluster box.

Between redshifts $z = 4$ and $z = 0$, the mean mass-weighted merger ratio for SMBH mergers in both the void and cluster is between $1 : 4$ and $1 : 5$. Our results can be compared to the mean mass-weighted merger ratio found by Oser et al. (2012) for individual galaxies with masses $4.5 \times 10^{10} h^{-1} M_\odot \lesssim M_* \lesssim 3.6 \times 10^{11} h^{-1} M_\odot$ from $z = 2$ to $z = 0$ using cosmological re-simulations. Our average values for the merger ratios are the same for $2 > z > 0$ for $4 > z > 0$, and are similar to the value of $\sim 1 : 5$ obtained by Oser et al. (2012) for galaxies. Our values are also roughly consistent with the range of values given for the median mass-weighted merger ratio of galaxy bulges in Hopkins et al. (2010), who studied galaxy bulges with masses $10^9 M_\odot \lesssim M_* \lesssim 10^{12} M_\odot$ at $z = 0$ using semi-empirical models. Since SMBH mergers are subsequent to galaxy mergers and SMBHs and their hosts are connected by scaling relations, the similarity of the results is not unexpected.

The mass distribution of central black holes that we obtain is shown in Figures 3 and 4. Figure 3 shows the fraction of black holes with mass greater than some M_\bullet , whereas Figure 4 shows the fraction of total black hole mass contained in black holes with mass $> M_\bullet$. As can be seen in Figure 3, the mass function of black holes is quite similar in the void and cluster boxes at all redshifts. The time evolution in the fraction of BHs with mass above some value is relatively small in both the void and cluster box. A slight trend can be seen in both boxes in which the fraction of high mass black holes first increases from

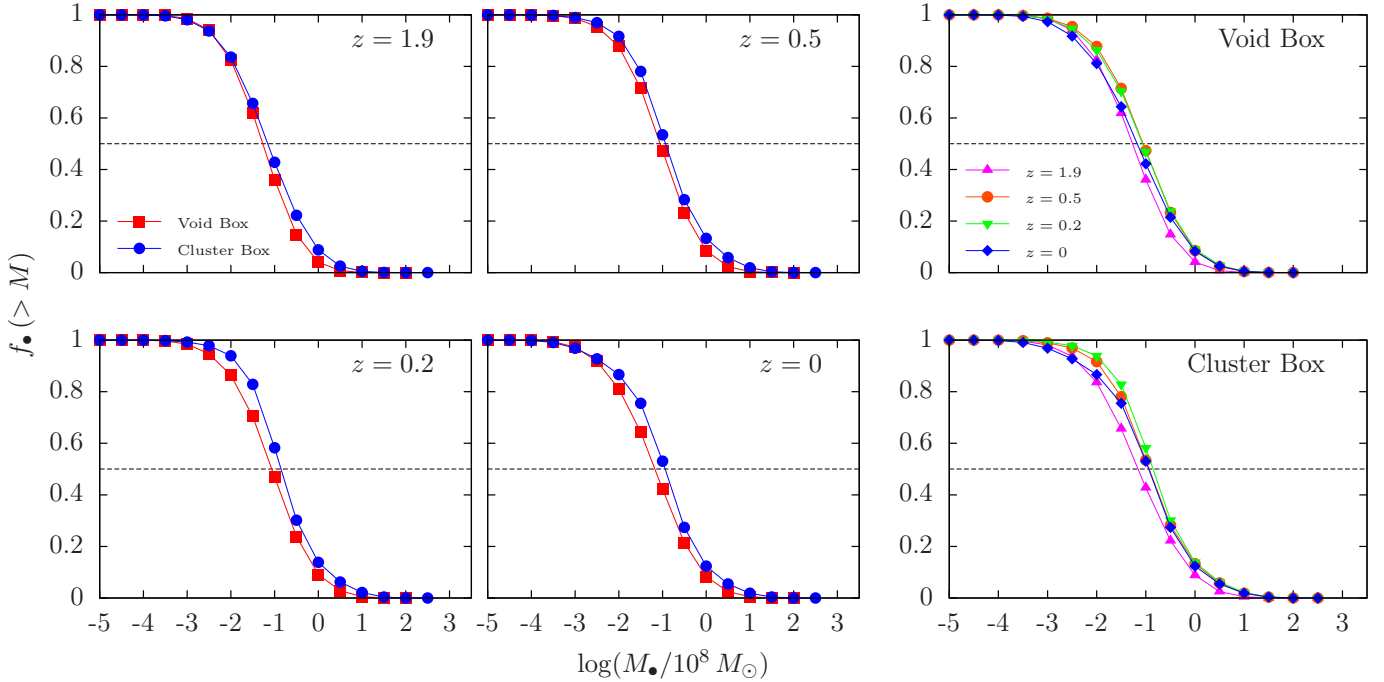


FIG. 3.— The fraction of central black holes with mass greater than some value M_\bullet . The left four panels show the fraction for the void and cluster boxes at $z = 1.9, 0.5, 0.2$ and 0 . The right two panels show the same curves, but grouped together for the void and cluster boxes, showing all four redshifts.

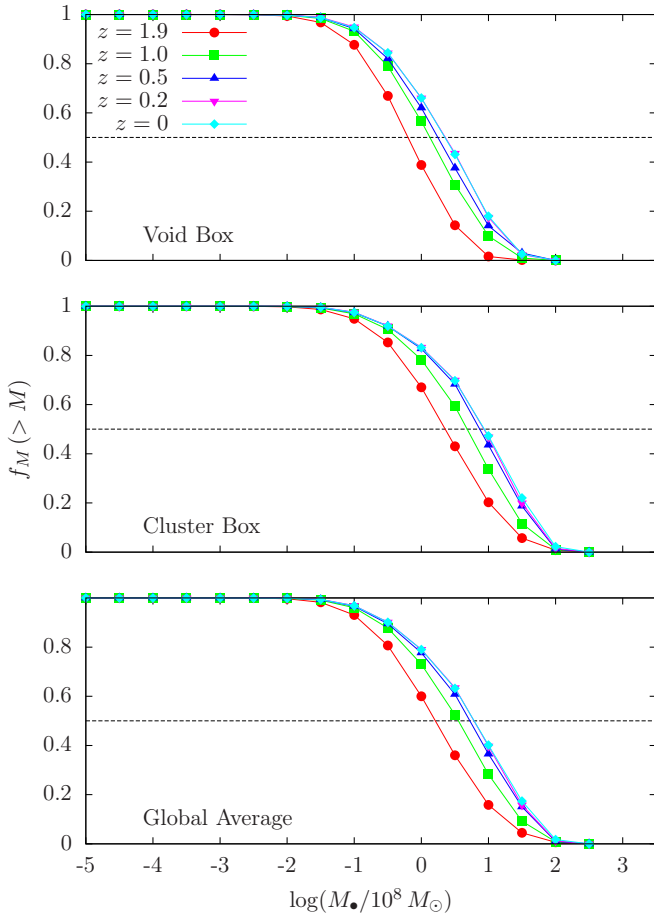


FIG. 4.— The fraction of total black hole mass contained in black holes with mass above some M_\bullet , shown at different redshifts.

$z = 1.9$ to $z \approx 0.2$, but then decreases between $z \approx 0.2$ and $z = 0$ as more low mass black holes are added to the population. As can be seen in Figure 4, the corresponding fraction of total mass contained in high mass black holes increases over time up to $z = 0.2$, and then stops. Figure 4 also shows that in both the cluster and void box, the total mass is overwhelmingly concentrated in the most massive black holes. At low redshifts, half of the mass is found in SMBHs with $M_\bullet \gtrsim 10^{8.5} M_\odot$ in the void, and in SMBHs with $M_\bullet \gtrsim 10^9 M_\odot$ in the cluster, despite the fact that such black holes are less than 5% of the total population in both boxes.

As described in §4.3, our simulation is known to significantly overproduce galaxies with large stellar mass in both the void and cluster boxes. It produces galaxies that are more massive than those observed, and these galaxies are also over-merged. It also has a tendency to underproduce galaxies with low stellar mass. Since the growth of our BHs closely follows the growth of their host galaxies by design, we would expect that the mass distribution of our SMBH population would be similarly biased toward high masses and away from low masses. Although we scale down the masses in the cluster and the void by a constant factor to match the observed stellar to dark matter mass ratio in these regions, and scale our “global average” so that the stellar mass density matches observations at $z = 0$, the shape of the BH population obtained with our model is likely to be skewed toward more massive black holes than in reality. Comparing the global average mass function we obtain at $z = 0$ to that from observations (Shankar et al. 2004; Marconi et al. 2004; Hopkins et al. 2007; Tundo et al. 2007), this indeed seems to be the case. Our mass function is a factor of ~ 5 lower than the mean of these observations for $10^7 M_\odot \lesssim M_\bullet \lesssim 10^9 M_\odot$. For $10^9 M_\odot \lesssim M_\bullet \lesssim 10^{10} M_\odot$,

our mass function is within the large 1σ range for some of the observations at these high masses, but the slope is noticeably much shallower than that observed in any of the four works; i.e., there is an excess of massive BHs.

The exact effects of these known shortcomings in our simulation on our model results are difficult to assess. The number of orbiting BHs and amount of orbiting mass predicted may be too high, since the dynamical friction timescale is larger for more massive galaxies, and especially since these timescales are calculated using the unscaled values of the galaxy masses. However, the dynamical friction timescale is also longer for satellite BHs with lower masses, which would be more plentiful were our SMBH mass function not skewed toward high masses. These have opposing effects on the predicted size of the orbiting BH population, and we cannot determine which is dominant. The fraction of BH mass from mergers (Figure 2) is also affected in opposing ways. The fact that the galaxies in the simulation suffer from over-merging implies that the central black holes do as well; however, the ratio of mass from mergers to total mass is also dependent on the shape of the BH mass function, which we know to be too low at low masses and too high at high masses. Other results will be affected by the over-merging as well; it increases the gravitational wave luminosity and strain we predict, as well as the number of BHs ejected by gravitational wave recoil, results that are described below.

The growth of SMBHs over time follows different trends in the void and cluster boxes. Figure 5 shows the rate of mass growth via accretion and mergers for SMBHs as a function of redshift. In both the cluster and void, accretion is the dominant source of growth for the total mass contained in SMBHs at all redshifts. Nevertheless, mergers become more important at recent times compared to accretion in both boxes. In the cluster, the accretion rate follows an overall downward trend with time, decreasing by a factor of ~ 3 since $z = 2$, while the merger rate stays roughly constant. In the void, the accretion rate increases slightly (by a factor of $\lesssim 2$) since $z = 2$, while the merger rate increases by about an order of magnitude (although the scatter is large).

Because mergers become more significant over time, in both the void and cluster the total black hole mass from mergers is added slightly later on average than that from accretion. In the void, half of the total mass from accretion at $z = 0$ has been added by $z \approx 0.6$, whereas for mergers half the mass has been added by $z \approx 0.4$. In the cluster, both half the merged and accreted mass are added before that in the void, and the difference between the two is larger; half the accreted mass is added by $z \approx 1.2$, while half the merged mass is added after $z \approx 0.8$. These SMBH growth trends parallel those of galaxies. Galactic mass assembly in the cluster tends to happen earlier than in the void, and in both the cluster and void mass buildup by accretion peaks at earlier times than by mergers (Lackner et al. 2012).

The connection between galaxy growth via galaxy mergers and BH growth via BH-BH mergers can also be seen in the top panel of Figure 6. This panel shows the number of mergers, weighted by the merger mass ratio, per central BH in a Hubble time. The merger history of the BH population approximately follows that of the galaxy population — which is to be expected, as

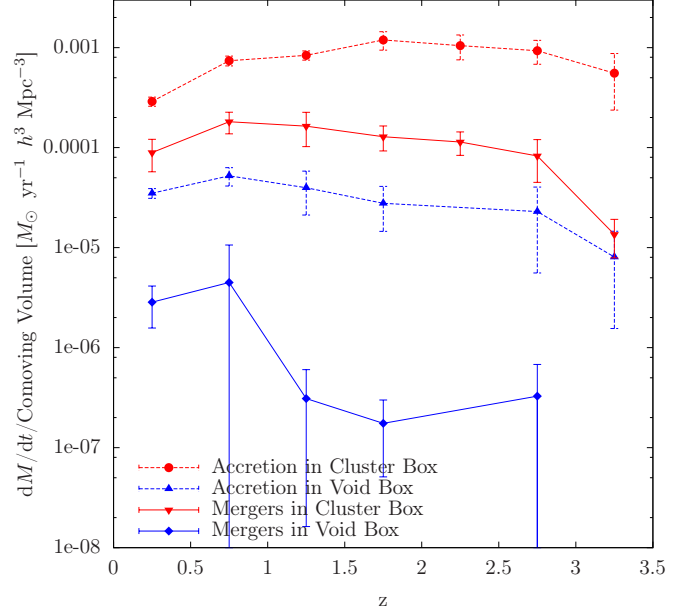


FIG. 5.— Growth rate of mass contained in central SMBHs per unit comoving volume from accretion and mergers. The dashed lines show the rate of mass increase due to gas accretion onto central black holes; the solid lines show the rate of mass increase due to mergers with smaller black holes. Red lines represent the cluster and blue lines represent the void.

BH mergers are subsequent to galaxy mergers, although sometimes delayed by dynamical friction. One can also see in this panel that in the cluster for $z > 0.5$, on average a central BH is predicted to experience the equivalent in mass increase of a $\sim 1 : 5$ to $\sim 1 : 4$ merger in a Hubble time. In the void, we predict an average of the equivalent of a $\sim 1 : 10$ merger in a Hubble time at all redshifts. While this implies a difference of ~ 2 in the growth due to mergers per central galaxy between the void and cluster, this is much less than the $\sim 1.5 - 3$ order-of-magnitude difference in the mass growth rate due to mergers per unit comoving volume seen in Figure 5.

The bottom panel of Figure 6 shows a related quantity, the fraction of central BHs ejected from their host galaxies in a Hubble time as a function of redshift. This follows the trend of the BH merger rate closely, since mergers cause ejections via gravitational wave recoil. The fraction ejected per Hubble time in the cluster is fairly constant over time at ~ 0.07 . In the void, the scatter is very large, but for $z < 1$ is ~ 0.04 .

Figure 7 shows the expected bolometric luminosity density emitted by the SMBHs due to gas accretion as a function of redshift for the cluster and void boxes as well as the global average. We assume an efficiency of $\epsilon = 0.1$, so that $L_{\text{bol}} = 0.1\dot{M}_{\text{acc}}c^2$. The quoted results can be scaled for other assumed values of the efficiency. Because the luminosity density is taken to be directly proportional to the rate of gas accretion, the shapes of the curves for the void and cluster boxes are the same as those for the accretion rate in Figure 5.

The expected global average luminosity output is roughly constant with redshift for $z > 0.5$, decreasing for the most recent times. In the lower panel, we compare our estimated global average luminosity to observations. Shown also is the observed QSO luminosity density from

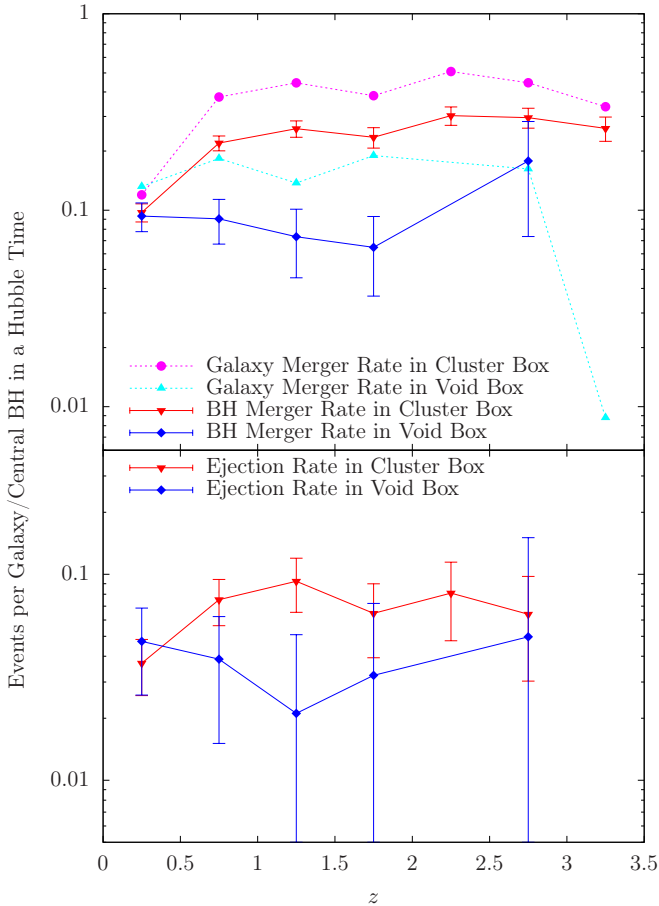


FIG. 6.— *Top Panel:* Merger rates of galaxies and SMBHs. The merger rates are expressed as the number of mergers per galaxy or central BH, weighted by merger ratio (e.g., a merger with ratio 1:2 is counted as 1/2), divided by the length of the simulation timestep and multiplied by the Hubble time at that redshift. The resulting value is a dimensionless number, giving the number of mergers weighted by ratio per Hubble time. Dotted lines represent the merger rate for galaxies and solid lines represent the merger rate for black holes.

Bottom Panel: The ejection rate of black holes from their host galaxies, expressed as the rate of ejections in each simulation timestep multiplied by the Hubble time, giving the number of ejections per Hubble time.

Hopkins et al. (2007), as well as $\epsilon \times 0.001 \times \text{SFRD} \times c^2$, using the observed star formation density (Madau diagram) from Hopkins & Beacom (2006). The observed QSO luminosity density has a roughly similar shape as the “expected trend” calculated from the observed SFRD, although it is somewhat lower. The luminosity density calculated from our model matches the overall magnitude of the observed luminosity density well, but does not replicate the shape. The insufficient downturn at low redshift in our result may be due to the fact that the cosmological simulation we use is known to especially overproduce stars at low z (Lackner et al. 2012), which would cause the proportional BH accretion rate to remain too high as well. Our scaling of the void to cluster is also quite simplistic, taking the void to cluster ratio to be constant with redshift. If this is not the case, the shape of our predicted trend would also change.

We also calculate the expected total energy density emitted in gravitational wave radiation as a result of BH-

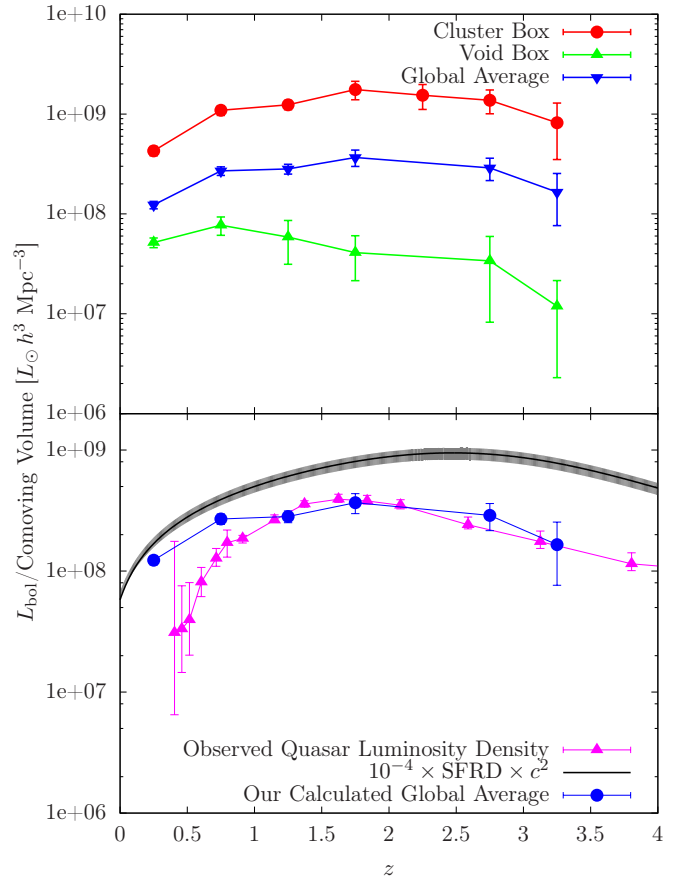


FIG. 7.— *Top Panel:* Estimated SMBH bolometric luminosity $E = 0.1\dot{M}_{acc}c^2$ per unit comoving volume due to gas accretion as a function of z for the void and cluster boxes and their weighted “global average”.

Bottom Panel: SMBH bolometric luminosity from different sources. In magenta is the observed QSO luminosity density from Hopkins et al. (2007). In black, for reference, is an estimate of the QSO luminosity density using the observed SFRD from Hopkins & Beacom (2006), based on an accretion rate onto the black hole of $10^{-3}\dot{M}_*$ and an efficiency factor of $\epsilon = 0.1$; the gray area represents an error of 1σ . The blue line is our calculation for the global average bolometric luminosity, also shown in the top panel.

BH mergers. The results are shown in Figure 8 for the global average. The luminosity follows a general increase with time, with the increase being significantly steeper for $z \gtrsim 2.5$. The gravitational wave luminosity, while very similar as a function of redshift to the rate of mass increase due to mergers (shown for the void and cluster separately in Figure 5), is not directly proportional, since the energy in emitted gravitational wave radiation is also dependent on the mass ratio of the merging black holes (see Equations 4-8).

Further, we calculate the gravitational wave strain produced by our population of black holes using the method described in Sesana (2012b). For a population of merging black hole binaries, where the black holes in each binary have masses M_1 and M_2 with $M_1 > M_2$, the characteristic amplitude of the gravitational wave signal h_c is given by

$$h_c^2(f) = \frac{4}{\pi f} \iiint dz dM_1 dq \frac{d^3n}{dz dM_1 dq} \frac{1}{1+z} \frac{dE_{gw}(\mathcal{M})}{d \ln f_r} \quad (11)$$

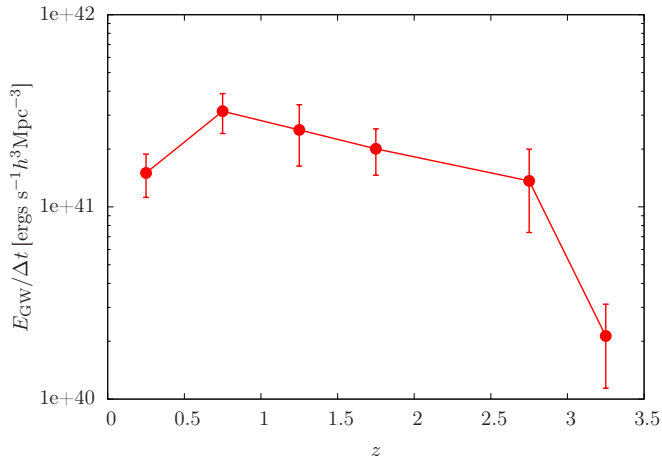


FIG. 8.— The global average gravitational wave luminosity density resulting from BH-BH mergers.

where the energy emitted per logarithmic frequency interval is

$$\frac{dE_{\text{gw}}}{d \ln f_r} = \frac{\pi^{2/3}}{3} \mathcal{M}^{5/3} f_r^{2/3} \quad (12)$$

where $\mathcal{M} = (M_1 M_2)^{3/5} / (M_1 + M_2)^{1/5}$ is the chirp mass of the binary and $f_r = (1 + z)f$ is the rest frame frequency of the gravitational radiation. The amplitude A is defined by

$$h_c(f) = A \left(\frac{f}{\text{yr}^{-1}} \right)^{-2/3}. \quad (13)$$

We find a global average strain amplitude of $\log A = -14.82 \pm 0.13$ (1σ error). This is below the current observational upper limit of $A = 6 \times 10^{-15}$ found by van Haasteren et al. (2011). Our result falls between the recent theoretical results of Sesana (2012b) and McWilliams et al. (2012); the former predicts a 3σ range of $1.1 \times 10^{-16} < A < 4.2 \times 10^{-15}$, while the latter predicts an expected strain of $A = 4.1 \times 10^{-15}$ with a 2σ lower limit of 1.1×10^{-15} . Our mean amplitude is higher than that of Sesana (2012b) and lower than that of McWilliams et al. (2012), but within 2σ of each.

5.1. Scatter in the $M_\bullet - M_*$ relation with mass

We divide the galaxies in the cluster box at $z = 0$ into bins in stellar mass, and fit separate $M_\bullet - M_*$ relations to each bin. We then calculate the scatter around the relation in each bin, σ , given by

$$\sigma^2 = \frac{\sum_i [\log_{10}(M_{\bullet,i}) - \alpha - \beta x_i]^2}{N_{\text{dof}}}, \quad (14)$$

where α and β are the coefficients of the fit. We plot the scatter for each bin in Figure 9. The relation is found to be tighter for black holes with larger masses. The void box, not shown here, exhibits a similar trend. Such a decrease in scatter with increasing M_* is the expected result of galaxy and subsequent BH-BH mergers, which tighten the $M_\bullet - M_*$ relation due to the central limit theorem (Hirschmann et al. 2010).

McConnell & Ma (2012) have done a similar calculation using a large data set of SMBHs with measured

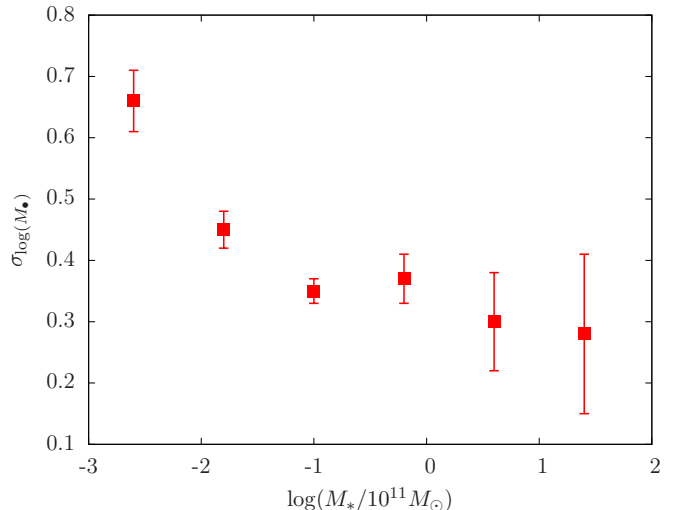


FIG. 9.— Scatter around the $M_\bullet - M_*$ relation as a function of M_* for the cluster box at $z = 0$. Points represent the scatter σ around a separate $M_\bullet - M_*$ relation fit in each bin. Error bars are one standard deviation of σ .

masses, and have obtained the scatter in various black hole-galaxy relations. While they were unable to find a significant decrease in the scatter as a function of mass when taking into consideration their large error bars, our results are nevertheless not inconsistent with their $M_\bullet - M_{\text{bulge}}$ relation.

5.2. Corrections to the Soltan argument

The Soltan argument for obtaining the accretion efficiency onto SMBHs depends on our ability to accurately measure the mass density in SMBHs at the present day. Since we observe such black holes only at the centers of galaxies, if some black holes have been ejected via gravitational wave recoil into the outer regions of the galaxy or out of the galaxy entirely, they will not be accounted for in the observed present day SMBH mass density. This is also true for those still in orbit after a merger. By taking into account such recoils in our model, we keep track of the fraction of mass in orbiting and ejected BHs that must be a correction to the Soltan argument. We report the values and 1σ errors for the logarithm of the mass and number fractions of orbiting and ejected BHs. We also give ranges for some of the results we obtain in multiple realizations of the model to emphasize that some of these results can vary widely between our different realizations and so should be taken as uncertain.

We find that at $z = 0$, in the void, the fraction of all BHs that are orbiting in the outskirts of their host galaxies is $\log f_n = -1.51 \pm 0.08$, with a range between our different realizations of -1.67 to -1.35 . The fraction of the total SMBH mass in orbiting black holes is $\log f_m = -2.47 \pm 0.21$, with a large range -2.92 to -2.12 . For the cluster, the amount of orbiting mass is much greater than in the void, as can already be seen in Figure 1. In fact, there is a very large population of orbiting SMBHs in the cluster, with $\log f_n = -0.39 \pm 0.01$ (about 40%) of BHs at $z = 0$ orbiting; however, most of these BHs are quite small (since less massive BHs have larger dynamical friction times), and so the fraction of mass in orbit is $\log f_m = -0.87 \pm 0.07$. It should be noted that these orbiting black holes are highly concentrated in the

most massive galaxies in our cluster box — as could be expected from the fact that a larger galaxy will have a longer dynamical friction time. In fact, approximately one third of all orbiting BHs in the cluster are found in the most massive galaxy. However, as mentioned above, our largest galaxies are considerably overmassive before scaling (the most massive being $M_* = 1.75 \times 10^{13} M_\odot$), and so the number and fraction by mass of orbiting BHs is probably exaggerated. Combining the cluster and void, these values correspond to a global average fraction of orbiting BHs of $\log f_n = -0.53 \pm 0.01$. The fraction of mass that is unaccounted for by observing galaxy centers is $\log f_m = -0.98 \pm 0.07$, with range -1.13 to -0.81 .

We also predict the fraction of black holes that are completely ejected from their host galaxies due to gravitational wave recoil. At $z = 0$, we find that in the void $\log f_n = -1.61 \pm 0.16$, where f_n is the fraction of all black holes that are not associated with any galaxy as a result of being ejected, equivalent to a loss of f_m of the total SMBH mass, where $\log f_m = -1.59 \pm 0.26$ (range -2.09 to -0.97). In the cluster $\log f_n = -1.38 \pm 0.06$ and $\log f_m = -1.39 \pm 0.20$ (range -1.85 to -0.94). It should be noted that while the fraction of black holes ejected is roughly constant for all our runs of the model, the fraction of mass ejected can vary significantly from one to the other, so the values we obtain are not very certain. The global average fraction of ejected BHs is $\log f_n = -1.43 \pm 0.05$, with a range -1.59 to -1.34 , and the fraction of mass ejected is $\log f_m = -1.41 \pm 0.17$ with a range -1.80 to -1.02 .

In combination, we predict that the total correction to the Soltan argument from both unaccounted-for orbiting and ejected BHs is within the range $1.6 - 15\%$ ($\log f_m$ from -1.80 to -0.81), with an average in the log of $\log f_m = -1.19 \pm 0.25$, or linearly $7.4 \pm 3.7\%$.

6. CONCLUSIONS

We have used the results of a set of hydrodynamic galaxy simulations of a void and cluster region in the universe to predict the evolution of the supermassive black holes that reside in these galaxies. We find significant late time growth of black holes in massive galaxies, although this growth is likely exaggerated in our simulation. Our predicted $M_\bullet - M_*$ relation agrees well with observed trends, as could be expected since our accretion rate onto the black holes was set to the observed value of $10^{-3} M_*$ (with some scatter). We calculate the contribution to the mass of the central black hole from accretion of gas and mergers with smaller black holes subsequent to the mergers of their two host galaxies. We find that in the cluster, the total BH mass from mergers is added later on average than the mass from accretion, with half the mass from accretion added before $z \approx 1.2$ and half the mass from mergers added after $z \approx 0.8$. In the void, half the total mass accreted onto the BH population is accreted before $z \approx 0.6$, but half the merged mass is added after $z \approx 0.4$. Mergers contribute a negligible amount to the mass of black holes with $M \lesssim 10^7 M_\odot$ in both the cluster and the void region. In the void, the number-weighted mean fraction of mass from mergers rises with black hole mass up to $\approx 8\%$ for BHs with $M_\bullet \gtrsim 10^{9.5} M_\odot$. In the cluster, the fraction from mergers reaches a maximum value of 20% for $M_\bullet \approx 10^9 M_\odot$, and decreases for larger mass BHs. For all BHs with some mass contribution

from mergers, the mean fraction of mass from mergers is larger in the cluster box than for galaxies of the same mass in the void box, although values for high-mass BHs have large scatter (Figure 2).

Additionally, we predict the mass in black holes orbiting in galaxies due to a galaxy-galaxy merger or gravitational wave recoil. While essentially negligible in the void box except for the most massive few galaxies ($M_* \sim 10^{11.5} M_\odot$), a significant amount of such mass is expected in cluster galaxies with $M_* \gtrsim 10^{11} M_\odot$ at $z = 0$. In the cluster, approximately 40% of the BHs and 14% of the BH mass is orbiting. We predict around 3 orbiting black holes on average for a galaxy in the cluster with unscaled mass around $10^{12} M_\odot$, or scaled mass around $2 \times 10^{11} M_\odot$. Such orbiting black holes are expected to produce observational signatures such as stellar tidal disruption flares that are off-center in the galaxy (Li et al. 2012; Liu & Chen 2013). They are also a candidate to explain observed ultra-luminous X-ray sources (Islam et al. 2004; Volonteri & Perna 2005; McWilliams et al. 2012).

We compute the expected energy emitted in gravitational wave radiation due to black hole mergers, shown in Figure 8. More energy is expected at smaller redshifts due to the larger amount of mass added via SMBH mergers during this time. We calculate the total strain amplitude from gravitational waves to be $\log A = -14.82 \pm 0.13$. We also compute the bolometric luminosity from accretion, shown in Figure 7, which is directly proportional to the mass increase from accretion. Our expected trend has roughly the same magnitude as the observed luminosity density ($\sim 2 \times 10^8 L_\odot h^3 \text{ Mpc}^{-3}$), but does not decrease sufficiently for $z < 1$ to match the observed trend.

We keep track of SMBHs that end up orbiting in a galaxy due to insufficient dynamical friction and SMBHs that are ejected from their hosts by gravitational wave recoils. These two populations would not be accounted for in attempts to calculate the local mass density of SMBHs by measuring the masses of black holes at the centers of galaxies. As such, they are a correction to the Soltan argument. We find that such SMBHs comprise between 1.6% and 15% of the total mass in SMBHs, with a mean of $7.4 \pm 3.7\%$.

We also find a modestly decreasing variance around the $M_\bullet - M_*$ relation with increasing mass in both the cluster and the void, shown for the cluster in Figure 9. This is a result of the fact that more massive BHs have undergone more mergers, which tighten the scaling relation due to the central limit theorem. Although current observational data are not sufficient to confirm or disprove the existence of this decrease in scatter, our results are consistent with the latest observational findings within the errors.

Therefore, late time mergers and their environment have interesting and observationally detectable consequences for the mass assembly history of supermassive black holes.

Computing resources were in part provided by the NASA High-End Computing (HEC) Program through the NASA Advanced Supercomputing (NAS) Division at Ames Research Center. This work is supported in part by grant NASA NNX11AI23G. This work was also sup-

ported by World Premier International Research Center Initiative (WPI Initiative), MEXT, Japan. A.K. ac-

knowledges the support of an NSF Graduate Research Fellowship.

REFERENCES

- Baker, J. G., Boggs, W. D., Centrella, J., et al. 2008, *ApJ*, 682, L29
- Baldry, I. K., Driver, S. P., Loveday, J., et al. 2012, *MNRAS*, 421, 621
- Barausse, E. 2012, *MNRAS*, 423, 2533
- Barausse, E., Morozova, V., & Rezzolla, L. 2012, *ApJ*, 758, 63
- Behroozi, P. S., Conroy, C., & Wechsler, R. H. 2010, *ApJ*, 717, 379
- Beifiori, A., Courteau, S., Corsini, E. M., & Zhu, Y. 2012, *MNRAS*, 419, 2497
- Bekenstein, J. D. 1973, *ApJ*, 183, 657
- Bell, E. F., McIntosh, D. H., Katz, N., & Weinberg, M. D. 2003, *ApJS*, 149, 289
- Bennert, V. N., Auger, M. W., Treu, T., Woo, J.-H., & Malkan, M. A. 2011, *ApJ*, 742, 107
- Binney, J., & Tremaine, S. 1987, *Galactic dynamics*
- Booth, C. M., & Schaye, J. 2011, *MNRAS*, 413, 1158
- Bournaud, F., Dekel, A., Teyssier, R., et al. 2011, *ApJ*, 741, L33
- Bournaud, F., Juneau, S., Le Floch, E., et al. 2012, *ApJ*, 757, 81
- Brinchmann, J., Charlot, S., White, S. D. M., et al. 2004, *MNRAS*, 351, 1151
- Brusa, M., Fiore, F., Santini, P., et al. 2009, *A&A*, 507, 1277
- Bryan, G. L. 1999, *Comput. Sci. Eng.*, Vol. 1, No. 2, p. 46 - 53, 1, 46
- Campanelli, M., Lousto, C., Zlochower, Y., & Merritt, D. 2007a, *ApJ*, 659, L5
- Campanelli, M., Lousto, C. O., Zlochower, Y., & Merritt, D. 2007b, *Physical Review Letters*, 98, 231102
- Cen, R. 2011a, *ApJ*, 741, 99
- . 2011b, *ApJ*, 742, L33
- . 2012a, *ApJ*, 753, 17
- . 2012b, *ApJ*, 748, 121
- . 2013, *ArXiv e-prints*
- Cen, R., Kang, H., Ostriker, J. P., & Ryu, D. 1995, *ApJ*, 451, 436
- Cen, R., Nagamine, K., & Ostriker, J. P. 2005, *ApJ*, 635, 86
- Cen, R., & Ostriker, J. P. 1992, *ApJ*, 399, L113
- Chen, C.-T. J., Hickox, R. C., Alberts, S., et al. 2013, *ArXiv e-prints*
- Ciotti, L., & Ostriker, J. P. 1997, *ApJ*, 487, L105
- Cisternas, M., Jahnke, K., Bongiorno, A., et al. 2011, *ApJ*, 741, L11
- Cole, S., Norberg, P., Baugh, C. M., et al. 2001, *MNRAS*, 326, 255
- Di Matteo, T., Colberg, J., Springel, V., Hernquist, L., & Sijacki, D. 2008, *ApJ*, 676, 33
- Di Matteo, T., Croft, R. A. C., Springel, V., & Hernquist, L. 2003, *ApJ*, 593, 56
- Diemand, J., Kuhlen, M., Madau, P., et al. 2008, *Nature*, 454, 735
- Dubois, Y., Devriendt, J., Slyz, A., & Teyssier, R. 2012, *MNRAS*, 420, 2662
- Dubois, Y., Gavazzi, R., Peirani, S., & Silk, J. 2013a, *ArXiv e-prints*
- Dubois, Y., Volonteri, M., & Silk, J. 2013b, *ArXiv e-prints*
- Eisenstein, D. J., & Hu, W. 1999, *ApJ*, 511, 5
- Ferrarese, L. 2002, *ApJ*, 578, 90
- Ferrarese, L., & Merritt, D. 2000, *ApJ*, 539, L9
- Ferrarese, L., Côté, P., Dalla Bontà, E., et al. 2006, *ApJ*, 644, L21
- Fitchett, M. J., & Detweiler, S. 1984, *MNRAS*, 211, 933
- Forté, J. C., Vega, E. I., & Faifer, F. 2012, *MNRAS*, 421, 635
- Gebhardt, K., & Thomas, J. 2009, *ApJ*, 700, 1690
- Gebhardt, K., Bender, R., Bower, G., et al. 2000, *ApJ*, 539, L13
- Gilli, R., Comastri, A., & Hasinger, G. 2007, *A&A*, 463, 79
- Greene, J. E., Peng, C. Y., & Ludwig, R. R. 2010a, *ApJ*, 709, 937
- Greene, J. E., Peng, C. Y., Kim, M., et al. 2010b, *ApJ*, 721, 26
- Gültekin, K., Richstone, D. O., Gebhardt, K., et al. 2009, *ApJ*, 698, 198
- Guo, Q., White, S., Li, C., & Boylan-Kolchin, M. 2010, *MNRAS*, 404, 1111
- Haardt, F., & Madau, P. 1996, *ApJ*, 461, 20
- Haehnelt, M. G., & Kauffmann, G. 2000, *MNRAS*, 318, L35
- Håring, N., & Rix, H.-W. 2004, *ApJ*, 604, L89
- Hausman, M. A., & Ostriker, J. P. 1978, *ApJ*, 224, 320
- Heckman, T. M., Kauffmann, G., Brinchmann, J., et al. 2004, *ApJ*, 613, 109
- Herrmann, F., Hinder, I., Shoemaker, D. M., Laguna, P., & Matzner, R. A. 2007, *Phys. Rev. D*, 76, 084032
- Hirschmann, M., Khochfar, S., Burkert, A., et al. 2010, *MNRAS*, 407, 1016
- Hopkins, A. M., & Beacom, J. F. 2006, *ApJ*, 651, 142
- Hopkins, P. F., & Hernquist, L. 2009, *ApJ*, 698, 1550
- Hopkins, P. F., Murray, N., & Thompson, T. A. 2009, *MNRAS*, 398, 303
- Hopkins, P. F., Richards, G. T., & Hernquist, L. 2007, *ApJ*, 654, 731
- Hopkins, P. F., Bundy, K., Croton, D., et al. 2010, *ApJ*, 715, 202
- Hu, J. 2009, *ArXiv e-prints*
- Islam, R. R., Taylor, J. E., & Silk, J. 2004, *MNRAS*, 354, 443
- Johansson, P. H., Burkert, A., & Naab, T. 2009, *ApJ*, 707, L184
- Joung, M. R., Cen, R., & Bryan, G. L. 2009, *ApJ*, 692, L1
- Kisaka, S., & Kojima, Y. 2010, *MNRAS*, 405, 1285
- Komatsu, E., Dunkley, J., Nolta, M. R., et al. 2009, *ApJS*, 180, 330
- Koppitz, M., Pollney, D., Reisswig, C., et al. 2007, *Physical Review Letters*, 99, 041102
- Kormendy, J., & Bender, R. 2011, *Nature*, 469, 377
- Kormendy, J., Bender, R., & Cornell, M. E. 2011, *Nature*, 469, 374
- Kormendy, J., & Richstone, D. 1995, *ARA&A*, 33, 581
- Lackner, C. N., Cen, R., Ostriker, J. P., & Joung, M. R. 2012, *MNRAS*, 425, 641
- Leauthaud, A., George, M. R., Behroozi, P. S., et al. 2012, *ApJ*, 746, 95
- Li, S., Liu, F. K., Berczik, P., Chen, X., & Spurzem, R. 2012, *ApJ*, 748, 65
- Li, Y., Haiman, Z., & Mac Low, M.-M. 2007, *ApJ*, 663, 61
- Lin, Y.-T., Brodwin, M., Gonzalez, A. H., et al. 2013, *ArXiv e-prints*
- Lin, Y.-T., Ostriker, J. P., & Miller, C. J. 2010, *ApJ*, 715, 1486
- Lin, Y.-T., Stanford, S. A., Eisenhardt, P. R. M., et al. 2012, *ApJ*, 745, L3
- Lippai, Z., Frei, Z., & Haiman, Z. 2009, *ApJ*, 701, 360
- Liu, F. K., & Chen, X. 2013, *ApJ*, 767, 18
- Lousto, C. O., & Zlochower, Y. 2011, *Physical Review Letters*, 107, 231102
- Lousto, C. O., Zlochower, Y., Dotti, M., & Volonteri, M. 2012, *Phys. Rev. D*, 85, 084015
- Madau, P., & Quataert, E. 2004, *ApJ*, 606, L17
- Maiolino, R., Gallerani, S., Neri, R., et al. 2012, *MNRAS*, 425, L66
- Malbon, R. K., Baugh, C. M., Frenk, C. S., & Lacey, C. G. 2007, *MNRAS*, 382, 1394
- Maoz, E. 1993, *MNRAS*, 263, 75
- Marconi, A., & Hunt, L. K. 2003, *ApJ*, 589, L21
- Marconi, A., Risaliti, G., Gilli, R., et al. 2004, *MNRAS*, 351, 169
- McConnell, N. J., & Ma, C.-P. 2012, *ArXiv e-prints*
- McLeod, K. K., & Bechtold, J. 2009, *ApJ*, 704, 415
- McWilliams, S. T., Ostriker, J. P., & Pretorius, F. 2012, *ArXiv e-prints*
- Menou, K., & Haiman, Z. 2004, *ApJ*, 615, 130
- Merloni, A., Rudnick, G., & Di Matteo, T. 2004, *MNRAS*, 354, L37
- Merloni, A., Bongiorno, A., Bolzonella, M., et al. 2010, *ApJ*, 708, 137
- Milosavljević, M., & Merritt, D. 2003, in *American Institute of Physics Conference Series*, Vol. 686, *The Astrophysics of Gravitational Wave Sources*, ed. J. M. Centrella, 201–210
- Moster, B. P., Naab, T., & White, S. D. M. 2013, *MNRAS*, 428, 3121
- Muzzin, A., Marchesini, D., Stefanon, M., et al. 2013, *ArXiv e-prints*
- Natarajan, P. 2004, in *Astrophysics and Space Science Library*, Vol. 308, *Supermassive Black Holes in the Distant Universe*, ed. A. J. Barger, 127
- Natarajan, P. 2011, *ArXiv e-prints*

- Netzer, H. 2009, MNRAS, 399, 1907
- Nipoti, C., Treu, T., Auger, M. W., & Bolton, A. S. 2009, ApJ, 706, L86
- Oser, L., Naab, T., Ostriker, J. P., & Johansson, P. H. 2012, ApJ, 744, 63
- Oser, L., Ostriker, J. P., Naab, T., Johansson, P. H., & Burkert, A. 2010, ApJ, 725, 2312
- O’Shea, B. W., Bryan, G., Bordner, J., et al. 2004, ArXiv Astrophysics e-prints
- Ostriker, J. P., Choi, E., Ciotti, L., Novak, G. S., & Proga, D. 2010, ApJ, 722, 642
- Park, K., & Ricotti, M. 2012, ApJ, 747, 9
- Peres, A. 1962, Physical Review, 128, 2471
- Pratt, G. W., Croston, J. H., Arnaud, M., & Böhringer, H. 2009, A&A, 498, 361
- Rashkov, V., & Madau, P. 2013, ArXiv e-prints
- Salvaterra, R., Haardt, F., & Volonteri, M. 2007, MNRAS, 374, 761
- Schnittman, J. D., & Buonanno, A. 2007, ApJ, 662, L63
- Sesana, A. 2012a, Advances in Astronomy, 2012
- . 2012b, ArXiv e-prints
- Shankar, F., Salucci, P., Granato, G. L., De Zotti, G., & Danese, L. 2004, MNRAS, 354, 1020
- Shankar, F., Weinberg, D. H., & Miralda-Escudé, J. 2009, ApJ, 690, 20
- Shields, G. A., Gebhardt, K., Salviander, S., et al. 2003, ApJ, 583, 124
- Sijacki, D., Springel, V., & Haehnelt, M. G. 2009, MNRAS, 400, 100
- Soltan, A. 1982, MNRAS, 200, 115
- Treister, E., Urry, C. M., & Virani, S. 2009, ApJ, 696, 110
- Tremaine, S., Gebhardt, K., Bender, R., et al. 2002, ApJ, 574, 740
- Tundo, E., Bernardi, M., Hyde, J. B., Sheth, R. K., & Pizzella, A. 2007, ApJ, 663, 53
- van Dokkum, P. G., Franx, M., Kriek, M., et al. 2008, ApJ, 677, L5
- van Haasteren, R., Levin, Y., Janssen, G. H., et al. 2011, MNRAS, 414, 3117
- van Meter, J. R., Miller, M. C., Baker, J. G., Boggs, W. D., & Kelly, B. J. 2010, ApJ, 719, 1427
- Volonteri, M. 2012, Science, 337, 544
- Volonteri, M., Madau, P., Quataert, E., & Rees, M. J. 2005, ApJ, 620, 69
- Volonteri, M., Natarajan, P., & Gültekin, K. 2011, ApJ, 737, 50
- Volonteri, M., & Perna, R. 2005, MNRAS, 358, 913
- Volonteri, M., Salvaterra, R., & Haardt, F. 2006, MNRAS, 373, 121
- Woo, J.-H., Treu, T., Malkan, M. A., & Blandford, R. D. 2008, ApJ, 681, 925
- Yoo, J., Miralda-Escudé, J., Weinberg, D. H., Zheng, Z., & Morgan, C. W. 2007, ApJ, 667, 813
- Yu, Q., & Tremaine, S. 2002, MNRAS, 335, 965
- Zhang, X., Lu, Y., & Yu, Q. 2012, ApJ, 761, 5